A METHOD BASED ON PARTICLE SWARM OPTIMIZA-TION TO RETRIEVE THE SHAPE OF RED BLOOD CELLS: A PRELIMINARY ASSESSMENT

Federico Caramanica[*]

Department of Information Engineering and Computer Science, University of Trento, Via Sommarive 14, Povo, Trento 38123, Italy

Abstract—The particle swarm optimization (PSO) algorithm, a global optimization technique based on cooperative swarming strategy, has been used to solve inverse scattering problem for red blood cells (RBCs) and detect possible anomalies. The inverse scattering problem is recast as an iterative optimization one by defining a suitable cost function. With this method is possible to estimate the morphological parameters of a red blood cell and to distinguish healthy RBCs from diseased ones. This work lays the basis for a new approach to make diagnosis. Preliminary numerical experiments show the potential effectiveness and the reliability of the proposed method as diagnostic tools.

1. INTRODUCTION

Recently, there has been growing interest in light scattering properties of biological tissues that are exploited in many diagnostic applications [1–3]. In particular, there is great attention in recovering the morphological parameters of a RBC from light scattering data.

   This problem can be formulated as an inverse light scattering problem (ILSP) [1, 4]. Similarly to other inverse problems, e.g., [5, 6], this kind of problem is non-linear and ill-posed: in other words, the ILSP for a single RBC does not have a closed form solution. Until now, there are two main strategies to solve the ILSP for a single biological particle. The first one distinguishes diseased cells with a methodology based on scattering statistics. This approach determines guidelines to identify healthy and diseased RBCs [1]. The second method, is an empirical approach based on a direct comparison of light scattering

patters with simulated ones from a reference database [7]. Both [1] and [7] depend on data that are used as reference and indirectly bias the ILSP results.

In this work, a new approach based on a stochastic global optimization technique called particle swarm optimizer (PSO) is presented. Recently, the PSO has been successfully adopted for the solution of complex electromagnetic problems [13–16]. The original ILSP is recast as a problem of optimization by defining a suitable cost function. Then, the cost function is minimized using the PSO and at the end of this iterative procedure, the morphological parameters of the investigated RBC are retrieved, allowing the diagnosis of possible diseases.

This article describes briefly the mathematical modeling of light scattering from a cell, i.e., the solution of the direct problem, and the cell shape model. Afterwards, the description of the PSO and the definition of the cost function used to recast the problem as an optimization one are introduced. Finally, some results are provided considering some of the most significative examples. This gives a preliminary assessment to the proposed inversion method and the basis for future practical application as diagnosis tool.

2. INVERSE LIGHT SCATTERING PROBLEM FOR RBC

In this section, the inverse scattering problem will be addressed and the methodology based on the PSO optimizer summarized.

To obtain scattering data of a single RBC, different methods have been used in the scientific literature: the finite-difference time-domain (FDTD) approach, the multilevel fast multipole algorithm (MLFMA) and others [4]. In this paper, we consider the discrete dipole approximation (DDA) [8, 9] that has shown good performance [3, 7, 8]. DDA is a method to compute scattering and absorption of electromagnetic wave by particles of arbitrary geometry and composition. In more detail, DDA replaces the solid particle by an array of M oscillating dipoles. Each dipole has an oscillating polarization in response both to an incident plane wave and to the electric fields due to all of the other dipoles in the array; the self-consistent solution for the dipole polarizations can be obtained as the solution to a set of coupled linear equations [7–9]. The optical cell shape model is the same of [7, 10], where a 4-parametric shape model has been proposed. The cell shape is described by as follows:

$$z^4 + \left[2R_4\left(\mathbf{p}\right)\rho^2 + R_2\left(\mathbf{p}\right)\right]z^2 + \rho^4 + R_1\left(\mathbf{p}\right)\rho^2 + R_3\left(\mathbf{p}\right) = 0 \quad (1)$$

where R_1, R_2, R_3 and R_4 depend on the morphological parameters of RBC, $\mathbf{p} = \{p_l, l = 1, \ldots, 4\} = \{D, h, b, c\}$ [7, 10]. D is the diameter of
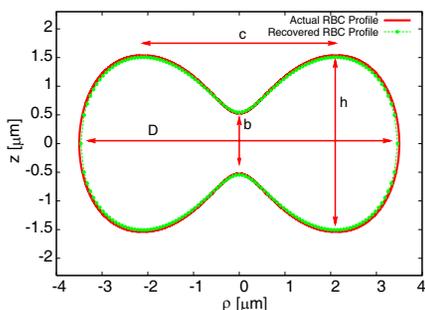
Figure 1. Comparison of the actual profile of the healthy RBC model vs the recovered profile after the PSO iterative procedure (z and ρ are cylindrical coordinates).

the RBC, h the maximum thickness, b the thickness at the center of the cell and c the diameter of a ring corresponding to the maximum thickness of a RBC (e.g., Fig. 1). The diameter D of a healthy RBC varies from $6.0\,\mu\text{m}$ to $9.0\,\mu\text{m}$ [3, 7]. If the diameter is larger than $9.0\,\mu\text{m}$, the RBC is called macrocyte. Conversely, a RBC diameter less than $6.0\,\mu\text{m}$ identifies a microcyte. The presence of microcyte may reveal disorder in iron metabolism or deficiencies in hemoglobin synthesis. Macrocytes may identify drug use, leukemia or other diseases [1].

This is the main reason for which it is important to develop an accurate and effective strategy to determine morphological parameters of a RBC and in particular its diameter D.

3. PSO-BASED INVERSION PROCEDURE

The goal of the proposed inversion procedure is to determine the vector of unknowns $\mathbf{x} = \{D, h, b, c\}$, that defines the morphological parameters of a RBC, defining a suitable cost fitness function and then minimizing it with an optimization algorithm. The cost function is formulated to estimate the error between the scattering data, obtained from the actual configuration $S_{11}^{actual}(\theta)$ and the current trial solution $S_{11}(\mathbf{x}, \theta)$, as shown in the following relation

$$\Psi(\mathbf{x}) = \frac{1}{\theta_{\max} - \theta_{\min}} \int_{\theta_{\min}}^{\theta_{\max}} \left[\log\left(S_{11}^{actual}(\theta) + 1\right) - \log(S_{11}(\mathbf{x}, \theta) + 1) \right] d\theta \tag{2}$$

where $\mathbf{x} = \{D, h, b, c\}$ is the n-th vector of unknowns, $\theta_{\min} = 0$ [deg] and $\theta_{\max} = 180$ [deg]. The above relation has been chosen following the guidelines described in [5, 14–17]. To minimize (2), there are

different approaches. Local searching techniques such as gradient based methods have a reduced computational burden, but can be trapped in local minima and can lead to false solutions. Consequently, we address to global optimization techniques. The most widely used are genetic algorithms (GAs) but in this work a swarm based methodology, namely the particle swarm optimizer (PSO) has been considered. The choice has been motivated by the advantages exhibited by PSO when compared to GAs [6]. The advantages are mainly concerned with the ability to control the convergence and avoid the stagnation of the optimization process, an easier implementation and calibration, and the exploitation of the cooperation among the trial solutions. However, it is worth noting that, for the "No Free Lunch Theorem" [11], an optimization strategy able to handle all the possible classes of problems does not exist. Moreover, for the problem at hand, the use of PSO gives better performance in respect to GA.

In PSO a swarm consists of a set of $n = 1, \ldots, N$ particles $\mathbf{x}_n^t = \{x_{n,k}^t, k = 1, \ldots, K\}$, being $t = 1, \ldots, T$. A position vector and a velocity one $(\mathbf{x}_n^t, \mathbf{v}_n^t)$ are associated to each particle of the swarm. In more detail, $\mathbf{v}_n^t$ models the capacity of the particle to fly, at iteration t-th, from a given position in the solution space $\mathbf{x}_n^t$ to the next one $\mathbf{x}_n^{t+1}$. The positions and the velocities of the N particles in the swarm are initialized by a random number generator. How well a trial solution solves the problem is determined by the evaluation of the cost function. At each iteration, position and velocity vectors of each particle are updated by the action of a force attracting them towards both their own previous positions $\mathbf{x}^{pb}$ and that of the entire swarm $\mathbf{x}^{gb}$: $\mathbf{v}_n^{t+1} = \alpha \mathbf{v}_n^t + C_1 \gamma_1 (\mathbf{x}_n^t - \mathbf{x}^{pb}) + C_2 \gamma_2 (\mathbf{x}_n^t - \mathbf{x}^{gb})$, where α is the inertia factor, C_1 and C_2 are constants called cognition and social acceleration, γ_1 and γ_2 are two randomly generated positive numbers between 0 and 1. The particle's position is then updated: $\mathbf{x}_n^{t+1} = \mathbf{x}_n^t + \mathbf{v}_n^{t+1}$. If the maximum number of iterations T is reached, or if the fitness of the best particle is within a predefined tolerance, the optimization process is stopped and the solution has been reached.

4. NUMERICAL RESULTS

The proposed inversion strategy to solve the ILSP is validated considering three different RBC profiles, each of them representing a significative example: a healthy RBC, a microcyte and a macrocyte whose actual morphological parameters are summarized in Table 1. This validation does not pretend to be exhaustive but has only the aim to give a preliminary assessment for a possible future use of this technique as diagnostic tools.

Table 1. Comparison of morphological RBC properties: actual vs recovered parameters (dimensions are in μm).

	RBC Type		
	Healty	Microcyte	Macrocyte
D_{actual}	7.00	5.00	12.00
$D_{recovered}$	6.93	4.98	11.89
h_{actual}	3.15	2.10	3.50
$h_{recovered}$	3.14	2.07	3.51
b_{actual}	1.05	0.90	1.50
$b_{recovered}$	1.09	0.86	1.46
c_{actual}	4.20	2.90	7.44
$c_{recovered}$	4.16	2.83	7.37

Concerning the PSO parameters, their values have been chosen following the guidelines provided in [13–15]. The number of particles in the swarm is set to $N = 6$, the maximum iterations $T = 200$ and the threshold $\eta = 10^{-1}$. The inertial weight α has been set equal to 0.4 to damp oscillations of the optimizer around the optimal solution and speed up the convergence rate, while C_1 and C_2 have been set equal to 2.0. The refractive index of the RBC is set $m_{RBC} = (1.406, 10^{-4})$ and the refractive index of the host medium, the blood plasma, is $m_{plasma} = (1.345, 0)$. As in [3], the imaginary part of the refractive index is considered negligible. The relative index of refraction becomes $\frac{m_{RBC}}{m_{plasma}} = 1.045$ while the the wavelength in the plasma is set to $\lambda = 0.497\,\mu m$ (in vacuum is $\lambda = 0.668\,\mu m$). The incident wave propagates along z-direction and the S_{11} element of the Mueller matrix is calculated [3]. The dependence of the S_{11} on the scattering angle θ in the x-z plane is computed considering the investigated RBC symmetric to the z axis, with the Euler angle $\beta = 0$. The authors of [7–9, 12] have introduced a rule for discretization that is widely considered sufficient to get accurate results: the minimum number of dipoles in the medium per lambda (dpl) is 10. To avoid inverse crime, the investigated RBC is discretized with $dpl = 12$ for the preliminary direct problem to obtain actual scattering data with DDA, while during numerical simulations in the inversion procedure, the synthetic data are generated with $dpl = 11$. The dpl value has been empirically chosen after a calibration procedure and the considered value represents a good compromise between computational burden and accuracy. The three test profiles show that the approach allows good estimation of the

unknown morphological parameters. This is confirmed by the relative error values (Fig. 3), defined for the parameter p_l

$$\Delta\left(p_l\right) = \frac{\left|p_l^{actual} - p_l^{recovered}\right|}{p_l^{actual}} \times 100\%, \quad l = 1, \ldots, 4 \qquad (3)$$

The geometrical profiles of the actual and the recovered healthy RBC are depicted in Fig. 1. The two profiles have an almost negligible difference and the maximum error is associated to the parameter b with a relative error 3.8%. In Figs. 2 and 3, the actual and the recovered profiles of healthy and microcyte RBC are traced in
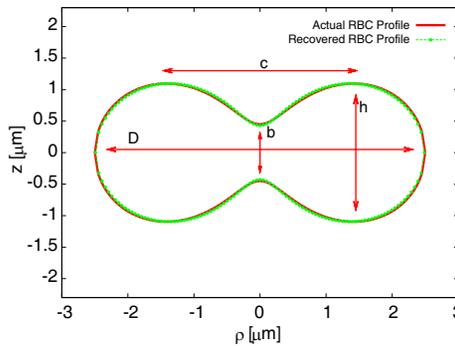
Figure 2. The actual profile of the microcyte RBC compared with the recovered one. The proposed PSO approach correctly identifies the descriptive parameters (z and ρ are cylindrical coordinates).
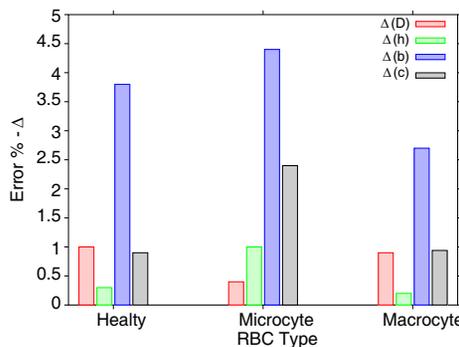
Figure 3. Relative errors in the reconstruction of the morphological parameters of the three RBCs. The relative error associated to diameter D, that allows to identify possible diseases, is at maximum equal to 1%.
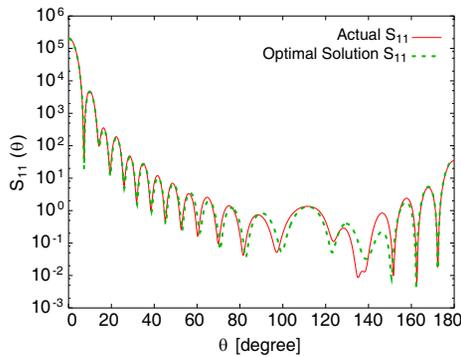
Figure 4. Microcyte test case: S_{11} values associated to the proposed solution generated after the iterative process.
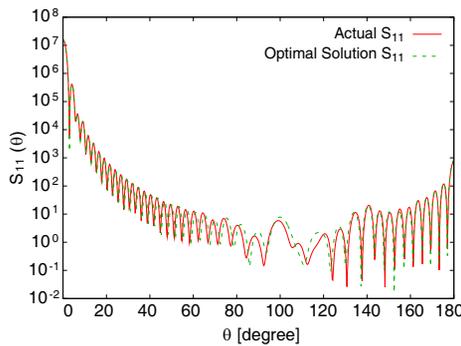
Figure 5. Macrocyte test case. For $\theta < 60$ [deg] and $\theta > 140$ [deg] the agreement between the two curves is satisfactory. In the interval 60 [deg] $< \theta < 140$ [deg] the matching is not perfect but anyway is considered acceptable.

cylindrical coordinates and compared.

In Fig. 4, there are the S_{11} values, depending on θ, for the actual and recovered microcyte test case. As previously stated, S_{11} is used to define the cost function and we can observe that for $\theta < 50$ [deg] and $\theta > 150$ [deg] there is a good agreement between the two curves. In the interval 50 [deg] $< \theta < 150$ [deg] the agreement is quite satisfactory. This is due to the difference of the morphological parameters (actual vs recovered) and the different number of *dpl* used in the direct and inverse procedure.

In a similar way, in Fig. 5, we have S_{11} values for the macrocyte RBC. Also in this third example, i.e., the macrocyte, the estimation

is satisfactory since the maximum relative error is 2.7% for RBC parameter b (Fig. 3).

5. CONCLUSION

In conclusion, we have applied the PSO algorithm to solve ILPS and retrieve the morphological profile of an RBC under investigation. In this preliminary assessment with ideal conditions and synthetic measures, the proposed approach has been able to correctly identify three different profiles of RBC and identify anomalies. In particular, the error associated to the diameter D is at maximum equal to 1% and this allows to correctly identify the different types of RBCs and make a diagnosis of possible diseases. Future work will be devoted to investigate the potentialities of the PSO approach in a more realistic scenario.

ACKNOWLEDGMENT

REFERENCES

1. Ergul, O., A. Arslan-Ergul, and L. Gurel, "Computational study of scattering from healthy and diseased red blood cells," *J. Biomed. Opt.*, Vol. 15, 045004, Aug. 2010.
2. Ergul, O., A. Arslan-Ergul, and L. Gurel, "Rigorous solutions of scattering problems involving red blood cells," *EuCAP*, 1–4, 2010.
3. Gilev, K. V., E. Eremina, M. A. Yurkin, and V. P. Maltsev, "Comparison of the discrete dipole approximation and the discrete source method for simulation of light scattering by red blood cells," *Opt. Express*, Vol. 18, 5681–5690, 2010.
4. Karlsson, A., J. He, J. Swartling, and S. Andersson-Engels, "Numerical simulations of light scattering by red blood cells," *IEEE Trans. on Biomed. Eng.*, Vol. 52, 13–18, Jan. 2005.
5. Caorsi, S., A. Massa, M. Pastorino, and M. Donelli, "Improved microwave imaging procedure for nondestructive evaluations of two-dimensional structures," *IEEE Trans. on Ant. and Propag.*, Vol. 52, 1386–1397, 2004.
6. Oliveri, G., F. Caramanica, and A. Massa, "Hybrid ADS-based techniques for radio astronomy array design," *IEEE Trans. on Ant. and Propag.*, Vol. 59, 1817–1827, Jun. 2011.

7. Yurkin, M. A., "Discrete dipole simulations of light scattering by blood cells," Ph.D. thesis, University of Amsterdam, 2007.

8. Yurkin, M. A., V. P. Maltsev, and A. G. Hoekstra, "The discrete dipole approximation for simulation of light scattering by particles much larger than the wavelength," *J. Quant. Spectrosc. Radiat. Transfer*, Vol. 106, 546–557, 2007.

9. "ADDA — light scattering simulator using the discrete dipole approximation," http://code.google.com/p/a-dda/, 2009.

10. Kuchel, P. W. and E. D. Fackerell, "Parametric-equation representation of biconcave erythrocytes," *Bulletin of Mathematical Biology*, Vol. 61, 209–220, 1999.

11. Wolpert, D. H. and W. G. Macready, "No free lunch theorems for optimization," *IEEE Trans. on Evolutionary Computation*, Vol. 1, 67–82, 1997.

12. Yurkin, M. A., K. A. Semyanov, P. A. Tarasov, A. V. Chernyshev, A. G. Hoekstra, and V. P. Maltsev, "Experimental and theoretical study of light scattering by individual mature red blood cells by use of scanning flow cytometry and a discrete dipole approximation," *Appl. Opt.*, Vol. 44, 5249–5256, 2005.

13. Martini, A., M. Donelli, M. Franceschetti, and A. Massa, "Particle density retrieval in random media using a percolation model and a particle swarm optimizer," *IEEE Ant. and Wireless Propag. Letters*, Vol. 7, 213–216, 2008.

14. Azaro, R., G. Boato, E. Zeni, M. Donelli, and A. Massa, "Design of Prefractal monopolar antenna for 3.4–3.6 GHz Wi-Max band portable devices," *IEEE Ant. and Wireless Propag. Letters*, Vol. 5, 116–119, 2006.

15. Azaro, R., F. DeNatale, E. Zeni, and M. Donelli, "Optimized design of a multifunction multiband antenna for automotive rescue system," *IEEE Trans. on Ant. and Propag.*, Vol. 54, 392–400, 2004.

16. Donelli, M., R. Azaro, L. Fimognari, and A. Massa, "A planar electronically reconfigurable Wi-Fi band antenna based on a parasitic microstrip structure," *IEEE Ant. and Wireless Propag. Letters*, Vol. 6, 623–626, 2007.

17. Donelli, M., S. Caorsi, F. De Natale, D. Franceschini, and A. Massa, "A versatile enhanced genetic algorithm for planar array design," *Journal of Electromagnetic Waves and Applications*, Vol. 18, No. 11, 1533–1548, 2004.